Bond and mode selectivity in the reaction of atomic chlorine with vibrationally excited CH_2D_2

Hans A. Bechtel, Zee Hwan Kim,[a] Jon P. Camden, and Richard N. Zare[b]
Department of Chemistry, Stanford University, Stanford, California 94305-5080

(Received 2 September 2003; accepted 13 October 2003)

The title reaction is investigated by co-expanding a mixture of Cl_2 and CH_2D_2 into a vacuum chamber and initiating the reaction by photolyzing Cl_2 with linearly polarized 355 nm light. Excitation of the first C–H overtone of CH_2D_2 leads to a preference for hydrogen abstraction over deuterium abstraction by at least a factor of 20, whereas excitation of the first C–D overtone of CH_2D_2 reverses this preference by at least a factor of 10. Reactions with CH_2D_2 prepared in a local mode containing two quanta in one C–H oscillator $|2000\rangle^-$ or in a local mode containing one quantum each in two C–H oscillators $|1100\rangle$ lead to products with significantly different rotational, vibrational, and angular distributions, although the vibrational energy for each mode is nearly identical. The $Cl+CH_2D_2|2000\rangle^-$ reaction yields methyl radical products primarily in their ground state, whereas the $Cl+CH_2D_2|1100\rangle$ reaction yields methyl radical products that are C–H stretch excited. The $HCl(v=1)$ rotational distribution from the $Cl+CH_2D_2|2000\rangle^-$ reaction is significantly hotter than the $HCl(v=1)$ rotational distribution from the $Cl+CH_2D_2|1100\rangle$ reaction, and the $HCl(v=1)$ differential cross-section (DCS) of the $Cl+CH_2D_2|2000\rangle^-$ reaction is more broadly side scattered than the $HCl(v=1)$ DCS of the $Cl+CH_2D_2|1100\rangle$ reaction. The results can be explained by a simple spectator model and by noting that the $|2000\rangle^-$ mode leads to a wider cone of acceptance for the reaction than the $|1100\rangle$ mode. These measurements represent the first example of mode selectivity observed in a differential cross section, and they demonstrate that vibrational excitation can be used to direct the reaction pathway of the $Cl+CH_2D_2$ reaction. © *2004 American Institute of Physics.* [DOI: 10.1063/1.1630961]

I. INTRODUCTION

An intuitive approach to reaction control with lasers is to excite vibrations that aid or hinder various reaction pathways.[1–3] These internal motions may be as simple as the stretching of a single bond or as complex as the collective motion of the entire molecule. The maximum vibrational control is expected to occur when these internal motions map directly onto the reaction coordinate. For diatomic molecules, the effects of vibrational excitation on reactivity are straightforward to predict and interpret because there is only one vibrational degree of freedom that couples to the reaction coordinate. Indeed, for late-barrier bimolecular reactions involving an atom and a diatom, Polanyi and co-workers[4–7] showed that vibrational excitation of the diatom is generally a more efficient means of overcoming the reaction barrier than translational energy. Extra vibrational degrees of freedom associated with polyatomic reagents, however, often complicate the simple concepts developed to explain atom–diatom reactions.

In a series of experiments involving the reaction of H, Cl, and O atoms with HOD the groups of Crim[8–13] and Zare[14–16] demonstrated that vibrational energy could be used to exert bond selectivity in reactions involving polyatomic reagents. In these experiments, vibrational excitation of the O–H stretch in HOD selectively enhanced the hydrogen-abstraction channel, whereas the excitation of the O–D stretch led to the deuterium-abstraction channel. Furthermore, the Crim group has monitored the $OH(v)$ product resulting from the reaction of H and Cl atoms with H_2O in two vibrational states, $|04\rangle^-$ and $|13\rangle^-$, where $|nm\rangle^{\pm}$ indicates the symmetric/antisymmetric combination of n and m quanta in the local mode stretch representation.[9,10] They found a marked production of $OH(v=0)$ from $H_2O|04\rangle^-$ and $OH(v=1)$ from $H_2O|13\rangle^-$, indicating that the initial excitation is retained in the nonreacting bond.

These demonstrations of mode- and bond-specific reactivity suggest a simple spectator paradigm, in which the vibrational energy in the nonreacting bond does not take part in the reaction. A growing body of experimental evidence indicates, however, that the vibration of the nonreacting bond does not always play the role of a spectator in vibrationally excited reactions. In the reaction of Cl+HCN, the groups of Crim[17,18] and Gericke[19,20] demonstrated that vibrational excitation of the C–H stretch led to significant vibrational excitation of the CN fragment, hinting that the CN fragment acts as a participant, not a spectator. Although the cause of this result is still under debate,[18–22] one proposed explanation is that the Cl+HCN reaction occurs via a complex that randomizes the prepared vibrational motion into other degrees of freedom. The randomization of the prepared vibrational motion caused by intramolecular vibrational redistri-

[a]Present address: Department of Chemistry, University of California, Berkeley, Berkeley, California 94720-1460.
[b]Author to whom correspondence should be addressed. Electronic mail: zare@stanford.edu

TABLE I. Energy levels of the vibrational modes of CH_2D_2.

Mode	Vibrational motion	Energy (cm^{-1})[a]	Fermi resonance
ν_1	CH_2 symmetric stretch	2975.49	$2\nu_3$
ν_2	CD_2 symmetric stretch	2146.4/2203.22	$2\nu_7$
ν_3	CH_2 scissor	1435.13	
ν_4	CD_2 scissor	1033.06	
ν_5	Torsion	1331.28	
ν_6	CH_2 antisymmetric stretch	3012.26	
ν_7	CH_2 rock	1091.22	
ν_8	CD_2 antisymmetric stretch	2234.7/2285.98	$\nu_4+\nu_9$
ν_9	CH_2 wag	1236.28	
	Local mode		
$\nu_2+\nu_8$	$\|0020\rangle^-$	4359	$2\nu_7$ and $\nu_4+\nu_9$
$\nu_1+\nu_6$	$\|2000\rangle^-$	5827/5879	$2\nu_3+\nu_6$
$2\nu_6$	$\|1100\rangle^-$	5999	

[a]The energies are from Ref. 27.

bution (IVR) during the reaction event could be a serious limitation to the general applicability of vibrational control to larger, more complex molecules, where the additional degrees of vibrational freedom make IVR more likely to occur.[23] The effectiveness of vibrationally controlled chemistry as applied to larger molecules, however, remains an unsettled issue, partly because of the scarcity of examples.

In a previous communication, we reported on the observed bond- and mode-selectivity in the reaction of atomic chlorine with various isotopomers of vibrationally excited methane.[24] Subsequently, Yoon *et al.*[25] observed bond-selectivity in the $Cl+CH_3D(2\nu_2)$ reaction, and Beck *et al.*[26] observed mode-selectivity in the reaction of vibrationally excited CH_2D_2 with Ni surfaces. In this article we investigate in detail the effects of vibrational excitation on the $Cl+CH_2D_2$ reaction by examining rotational distributions and differential cross sections (DCSs) of the products. We compare the product energy disposal and reactive scattering dynamics of two nearly isoenergetic states involving the first overtone of the C–H stretch of CH_2D_2, and we measure the branching ratio in the bond-selective reaction:

$$Cl+CH_2D_2(\nu) \rightarrow HCl+CHD_2 \quad (1a)$$

$$Cl+CH_2D_2(\nu) \rightarrow DCl+CH_2D \quad (1b)$$

in which the first overtone of the C–H or C–D stretch in CH_2D_2 is excited.

Dideuteromethane (CH_2D_2) is an asymmetric top with nine vibrational modes, eight of which are infrared active. Consequently, the infrared spectrum is highly congested and many of the lines are overlapped;[27] Table I lists the infrared active normal modes and their fundamental frequencies. In this article we examine the effects of the first overtone of the antisymmetric C–H stretch ($2\nu_6$) at 5999 cm^{-1} and the symmetric and antisymmetric C–H stretch combination ($\nu_1+\nu_6$) at 5879 cm^{-1}.[27] These two C–H stretch overtones have approximately the same energy, but correspond to different nuclear motions. The $2\nu_6$ motion corresponds to one quantum of energy in each C–H oscillator, whereas the $\nu_1+\nu_6$ state corresponds to two quanta of energy in one C–H oscillator.[28] Thus, in the local mode basis, $2\nu_6$ corresponds to $|1100\rangle$ and $\nu_1+\nu_6$ corresponds to $|2000\rangle^-$, where $|H_1H_2D_1D_2\rangle^{\pm}$ indicates the symmetric/antisymmetric combination of the individual C–H and C–D stretching oscillators. For simplicity of notation and reasons that will be discussed later, we will use the local mode representation in what follows; however, it must be cautioned that the eigenstates are not pure local mode states. The ν_1 state is perturbed by a stretch–bend Fermi resonance with the CH_2 deformation overtone, $2\nu_3$, which occurs about 100 cm^{-1} lower in energy.[27] Consequently, the $\nu_1+\nu_6$ state is also blueshifted. The antisymmetric CH stretch ν_6 is unperturbed by a Fermi resonance.

We also examine the C–D symmetric and antisymmetric stretch combination $\nu_2+\nu_8$ at 4359 cm^{-1}, which corresponds to the $|0020\rangle^-$ state in the local mode basis. The CD stretching fundamentals both experience major Fermi resonance perturbations, ν_2 with $2\nu_7$ (CH_2 rock) and ν_8 with $\nu_4+\nu_9$ (CD_2 scissor and CH_2 wag). We attempted to examine the $2\nu_8(|0011\rangle)$ overtone as assigned by Duncan and Law,[27] but could find no evidence for CD reactivity.

Figure 1 displays the relevant energetics of the $Cl+CH_2D_2$ reaction. Information taken from the Physical Chemistry Reference Data[29] indicates that the related reaction $Cl+CH_4 \rightarrow HCl+CH_3$ is slightly endothermic: $\Delta H = 600$ cm^{-1} (1.7 kcal/mol). Using the harmonic approximation to correct for changes in zero-point energies, the $Cl+CH_2D_2$ reaction has an endothermicity of ~670 cm^{-1} for the H-abstraction channel and ~700 cm^{-1} for the D-abstraction channel. Experimental measurements of the $Cl+CH_4$ reaction indicate that the activation energy is 800–1300 cm^{-1} (2.4–3.6 kcal/mol),[30] whereas *ab initio* calculations find the barrier to be in the 1300–1900 cm^{-1} (3.6–5.5 kcal/mol) range.[31] Recent calculations of the $Cl+CH_2D_2$ reaction show that the activation energy is 1800 cm^{-1} (5.2 kcal/mol) for the H-abstraction channel and 2200 cm^{-1} (6.3 kcal/mol) for the D-abstraction channel.[32] The combination of translational and vibrational energy is used to overcome the reaction barrier. Photolysis of Cl_2 at 355 nm provides ~1400 cm^{-1} of translational energy in the center of mass frame, and excitation of the overtone of the C–H stretch provides ~6000 cm^{-1} of vibrational energy, whereas excitation of the overtone of the C–D stretch provides ~4400 cm^{-1} of vibrational energy. Owing to the relatively high energies employed in this reaction, significant vibrational excitation in both the HCl and methyl radical products is possible, as shown in Fig. 1.

II. EXPERIMENT

The methods and experimental apparatus have been explained in detail previously,[33,34] therefore, only the primary features are presented here. A 1:4:5 mixture of molecular chlorine (Matheson, research grade, 99.999%), dideuteromethane (Cambridge Isotopes, 98%), and helium (Liquid Carbonic, 99.995%) is supersonically expanded into the extraction region of a linear time-of-flight (TOF) spectrometer

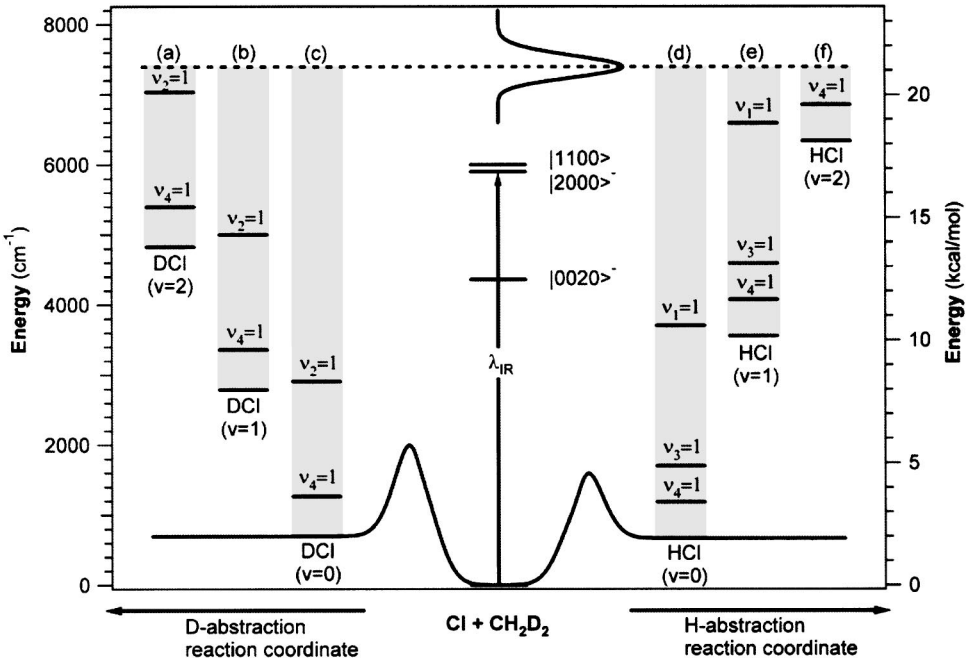

FIG. 1. Energy level diagram for the reaction of Cl with CH_2D_2. The left-hand arrow indicates the D-abstraction channel and the right-hand arrow indicates the H-abstraction channel. The $|1100\rangle$, $|2000\rangle^-$, and $|0020\rangle^-$ vibrational states of CH_2D_2 are prepared by direct overtone absorption of an IR photon (λ_{IR}). Photolysis of Cl_2 at 355 nm provides 1400 cm^{-1} of collision energy with an energy spread represented by a Gaussian distribution as determined from the formulas of van der Zande *et al.* (Ref. 56) assuming a translational temperature of 15 K. The different product channels are presented in gray squares: (a) $DCl(v=2)+CH_2D(\nu)$; (b) $DCl(v=1)+CH_2D(\nu)$; (c) $DCl(v=0)+CH_2D(\nu)$; (d) $HCl(v=0)+CHD_2(\nu)$; (e) $HCl(v=1)+CHD_2(\nu)$; and (f) $HCl(v=2)+CHD_2(\nu)$.

having a Wiley–McLaren configuration. The vibrational state of CH_2D_2 is prepared by direct IR overtone excitation, and the reaction is initiated by the photolysis of Cl_2 with linearly polarized 355 nm light. At this wavelength, monoenergetic Cl atoms are produced primarily in the ground state ($^2P_{3/2}$) with an anisotropy parameter $\beta=-1$.[35] After a 60–100 ns time delay, the HCl or CHD_2/CH_2D products are state selectively ionized by $2+1$ resonance-enhanced multiphoton ionization (REMPI), separated by mass, and detected by microchannel plates. The reactive signal from vibrationally excited methane is separated from the reactive signal from ground-state methane by modulating the IR light and subtracting the resultant signals on a shot-by-shot basis.

The IR radiation is generated in a two-step process involving difference-frequency mixing and optical parametric amplification. For the C–H overtone studies, mid-IR light at $\lambda=2.9$ μm is first generated via difference-frequency mixing by combining the 1064 nm fundamental of an Nd:YAG laser (Continuum PL9020) with the output of a dye laser (Continuum ND6000, Exciton LDS765) in a lithium niobate ($LiNbO_3$) crystal. The mid-IR radiation is then parametrically amplified in a second $LiNBO_3$ crystal that is pumped by another 1064 nm beam to produce approximately 15 mJ of the 1.7 μm (signal) light. For the C–D overtone studies, the required 2.2 μm radiation is generated directly by difference-frequency mixing (Exciton LDS751) and amplified in the second $LiNBO_3$ crystal. The 355 nm photolysis beam is generated by frequency tripling the output of the Nd:YAG laser, and the probe light for REMPI is generated by frequency doubling the fundamental of a dye laser output (Quanta Ray DCR-2A, Lambda Physik FL 2002, Exciton LD489 or DCM/LDS698) in a BBO crystal. The $HCl(v=1)$ products are detected via the $F\,^1\Delta-X\,^1\Sigma(1,1)$ and the $E\,^1\Sigma-X\,^1\Sigma(0,1)$ transitions,[36,37] and the methyl radical products are detected by the $3p\,^2B_1-X\,^2B_1$ transition.[38] The $HCl(v=0)$ products are not studied because of significant $HCl(v=0)$ background, resulting from prereactions of Cl_2 with impurities in the CH_2D_2 sample. Although the $HCl(v=2)$ reaction signal from the $Cl+CH_2D_2|2000\rangle^-$ reaction is observed via the $F\,^1\Delta-X\,^1\Sigma(1,2)$ transitions, poor signal to noise ratio prevents us from obtaining rotational distributions or TOF measurements. The $HCl(v=2)$ reaction signal from the $Cl+CH_2D_2|1100\rangle$ reaction is not observed.

A photoelastic modulator (PEM-80, Hinds International Inc.) flips the direction of the photolysis laser polarization between parallel and perpendicular to the TOF axis on an every-other-shot basis in order to obtain the isotropic $\mathbf{I}_{iso}=\mathbf{I}_{\parallel}+2\mathbf{I}_{\perp}$ and anisotropic $\mathbf{I}_{aniso}=2(\mathbf{I}_{\parallel}-\mathbf{I}_{\perp})$ components of the core-extracted TOF profiles. The isotropic TOF profile removes any dependence on the photolysis spatial anisotropy and provides a direct measurement of the speed distribution. These profiles are analyzed and converted into differential cross sections (DCSs) by a method similar to that of Simpson *et al.*[34] The anisotropic TOF profiles are analyzed to estimate the amount of internal energy deposited into the co-product by a method similar to Kim *et al.*[39] Because the vibrational state of CH_2D_2 is prepared by polarized light, it is possible to align the CH_2D_2 reactants, which could have an effect on the product speed distributions. Changing the polarization of the IR light, however, did not affect the mea-

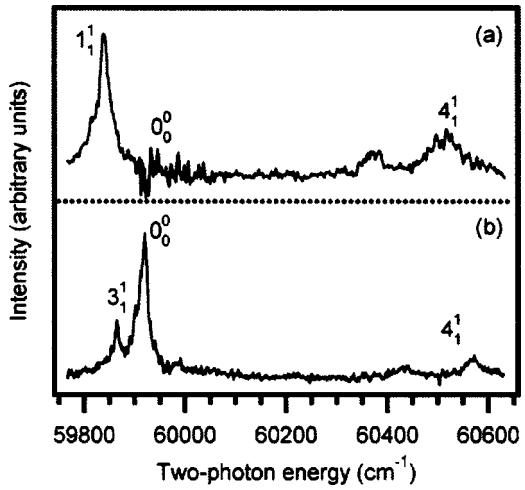

FIG. 2. $2+1$ REMPI spectrum of the CHD_2 product for the reaction of Cl with (a) $CH_2D_2|1100\rangle$ and (b) $CH_2D_2|2000\rangle^-$. (a) The spectrum from the $CH_2D_2|1100\rangle$ reaction has intensity in the 1_1^1 band and little intensity in the 0_0^0 band, indicating that the CHD_2 product is C–H stretch excited. (b) The spectrum from the $CH_2D_2|2000\rangle^-$ reaction has no intensity in the 1_1^1 band, but large intensity in the 0_0^0 band, indicating that the CHD_2 product is in the ground state.

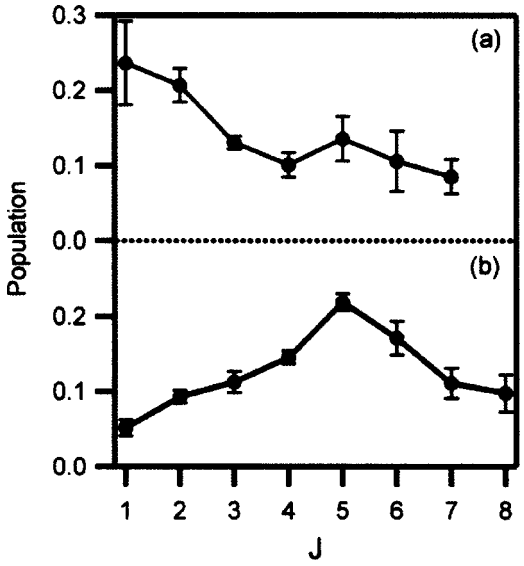

FIG. 3. Rotational distribution of the $HCl(v=1)$ product for the reaction of Cl with (a) $CH_2D_2|1100\rangle$ and (b) $CH_2D_2|2000\rangle^-$. The error bars represent σ_{n-1} of replicate measurements.

sured TOF profiles within our signal to noise. Thus, we have neglected the effect of reagent alignment in our data analysis.

III. RESULTS

A. Vibrational distributions of the CHD_2 products

Figure 2 shows the methyl radical REMPI spectra from the two reactions:

$$Cl+CH_2D_2|1100\rangle \rightarrow HCl+CHD_2, \tag{2a}$$

$$Cl+CH_2D_2|2000\rangle^- \rightarrow HCl+CHD_2. \tag{2b}$$

Vibrational band assignments are listed in Table II and are made according to the $3p\,^2B_1-X\,^2B_1$ REMPI scheme of Brum *et al.*[38] The peak at 59 840 cm^{-1} in Fig. 2(a) is redshifted 80 cm^{-1} from the 0_0^0 band and is assigned to the 1_1^1 band (C–H stretch) based on the expected 76 cm^{-1} redshift calculated from the experimental value of the ground-state CHD_2 radical,[40] $\nu_1=3116.2$ cm^{-1}, and the value of the excited-state CHD_2 radical, $\nu_1=3040$ cm^{-1}, obtained from the 1_0^1 band in the REMPI spectrum.[38] The location of the CH_3 1_1^1 band in this area of the REMPI spectrum validates this assignment.[41] The two peaks in the 4_1^1 region of Fig. 2(b) are in excellent agreement with literature values.[38] In Fig. 2(a), however, the maxima of these peaks are redshifted from the literature values by ~60 cm^{-1}. We believe the peak located at 59 865 cm^{-1} and redshifted 55 cm^{-1} from the 0_0^0 band is the 3_1^1 band, based on the assignment made by Zhou *et al.*[42]

TABLE II. Band maxima observed in the $3p\,^2B_1-X\,^2B_1$ $2+1$ REMPI spectrum of the CHD_2 radical from the $Cl+CH_2D_2|1100\rangle$ and $Cl+CH_2D_2|2000\rangle^-$ reactions.

Transition	Two-photon energy (cm^{-1})		
	$\|1100\rangle$	$\|2000\rangle^-$	Literature
1_1^1	59840	c	c
3_1^1	c	59865	59866[a]
0_0^0	c	59920	59920[b]
	60378	60440	60440[b]
4_1^1	60515	60575	60575[b]

[a]Assigned in Ref. 42.
[b]Literature values are from Ref. 38 and are reported in vacuum.
[c]Unobserved transition.

From Fig. 2, it is apparent that the methyl radical vibrational state distributions from the $Cl+CH_2D_2|1100\rangle$ and $Cl+CH_2D_2|2000\rangle^-$ reactions are quite different. The $Cl+CH_2D_2|1100\rangle$ reaction yields methyl radical products having C–H stretch excitation but with little to no ground-state products, whereas excitation of the $Cl+CH_2D_2|2000\rangle^-$ reaction produces predominantly ground-state methyl radicals.[24] Both reactions also produce non-negligible amounts of the methyl products in the out-of-plane large amplitude bending (OPLA) mode ν_4, and the $Cl+CH_2D_2|2000\rangle^-$ reaction produces methyl products in the CD_2 scissor mode ν_3. Vibrational branching ratios, however, could not be determined because of significant predissociation and the unknown Franck–Condon factors for the CHD_2 REMPI scheme. The energy difference between the $CH_2D_2|1100\rangle$ and $CH_2D_2|2000\rangle^-$ modes is only 120 cm^{-1}, which is less than 2% of the total available energy (7400 cm^{-1}). Consequently, we believe that the difference in prepared vibrational motion, not the energy, causes the difference in the methyl radical vibrational distribution.

B. Rotational distributions of $HCl(v=1)$ products

Figure 3 shows the rotational distributions of the $HCl(v=1)$ products from the reactions of the Cl-atom with $CH_2D_2|1100\rangle$ and $CH_2D_2|2000\rangle^-$, which have been obtained by detecting the H^+ fragment from the $E\,^1\Sigma-X\,^1\Sigma(0-1)$ Q-branch members and the $H^{35}Cl^+$ signal from the $F\,^1\Delta-X\,^1\Sigma(1,1)$ R-branch members. The correc-

tion factors of Simpson *et al.*[34] are used to convert from signal intensity to population and include the effects of fragmentation when detecting the H^+ fragment from the $E\,^1\Sigma - X\,^1\Sigma(0-1)$ Q-branch members. Uncertainties in these correction factors arising from different laser focusing conditions between our measurements and those of Simpson *et al.*[34] may lead to small errors in the quantitative analysis of the $HCl(v=1)$ rotational distributions, but they should not affect the qualitative comparison between the two vibrationally excited reactions because both rotational distributions were taken under identical conditions.

As indicated in Fig. 3, the $HCl(v=1,J)$ rotational distribution of the $Cl+CH_2D_2|1100\rangle$ reaction is strikingly different than the $HCl(v=1,J)$ rotational distribution of the $Cl+CH_2D_2|2000\rangle^-$ reaction, despite the two vibrations having approximately the same energy. The distribution from the $Cl+CH_2D_2|1100\rangle$ reaction decreases monotonically from $J=1$, whereas the distribution from the $Cl+CH_2D_2|2000\rangle^-$ reaction peaks at $J=5$ before dying off. Both distributions, however, are rotationally cold. For the $Cl+CH_2D_2|1100\rangle$ reaction, the average energy in rotation is $200\pm50\ cm^{-1}$, which is only ~5% of the available energy ($3800\ cm^{-1}$). The $Cl+CH_2D_2|2000\rangle^-$ reaction has more rotational energy, $340\pm50\ cm^{-1}$, but is still less than 9% of the available energy. Cold rotational distributions have been observed previously in hydrogen abstraction reactions of atomic chlorine with hydrocarbons,[34,39,43–45] and their significance will be discussed below.

Because more energy is localized in a single C–H oscillator, we might expect to observe an increase in reactivity for the $Cl+CH_2D_2|2000\rangle^-$ reaction over the $Cl+CH_2D_2|1100\rangle$ reaction. Detection of the $HCl(v=1)$ and $HCl(v=2)$ products suggests that there is indeed an increased reactivity for the $Cl+CH_2D_2|2000\rangle^-$ reaction, but a quantitative comparison is limited by the substantial beam walk of our IR source over the $\sim120\ cm^{-1}$ region separating the $CH_2D_2|2000\rangle^-$ and $CH_2D_2|1100\rangle$ bands. Beck *et al.*[26] recently quantified the increase in reactivity of $CH_2D_2|2000\rangle^-$ over $CH_2D_2|1100\rangle$ in reactions with Ni surfaces to be as much as a factor of five. Crim and co-workers[9,10] have also observed an increase in reactivity of $H_2O|03\rangle^-$ over $H_2O|12\rangle^-$ in reactions with fast H-atoms. These results clearly exclude the use of statistical models to correctly describe the mechanisms of these reactions because the vibrational modes are nearly isoenergetic.

C. Angular distributions of HCl($v=1$) products

TOF profiles of $HCl(v=1,J)$ products were obtained using members of the R and S branches of the $F\,^1\Delta - X\,^1\Sigma(1,1)$ band. Figure 4 shows representative TOF profiles of the HCl ($v=1$, $J=0/2$) products from the $Cl+CH_2D_2|1100\rangle$ and $Cl+CH_2D_2|2000\rangle^-$ reactions, obtained on the overlapped $S(0)$ and $R(2)$ lines. The TOF profiles differ dramatically for the $Cl+CH_2D_2|1100\rangle$ and $Cl+CH_2D_2|2000\rangle^-$ reactions, which can be related to the different product angular distributions, as seen below. This difference is quantified by fitting the TOF profiles with a set of basis functions generated by

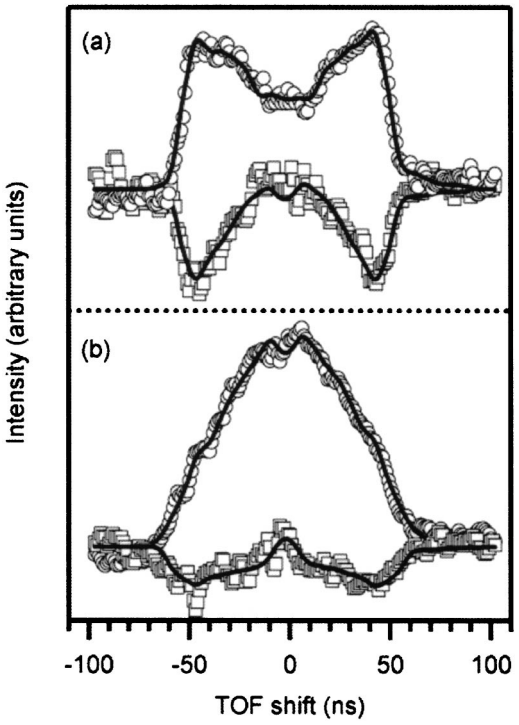

FIG. 4. Isotropic $I_{iso}=I_\parallel+2I_\perp$ and anisotropic $I_{aniso}=2(I_\parallel-I_\perp)$ components of the core-extracted TOF profile of the $HCl(v=1,J=0/2)$ product from the reaction of Cl with (a) $CH_2D_2|1100\rangle$ and (b) $CH_2D_2|2000\rangle^-$. The open circles are the measured isotropic TOF profiles, the open squares are the measured anisotropic TOF profiles, and the solid lines are the results of the fit.

Monte Carlo simulation.[33] The analysis provides the lab frame speed distributions of the $HCl(v=1)$ products, and Fig. 5 presents the results.

These speed distributions can be converted into DCSs with knowledge of the internal energies of the CHD_2 co-

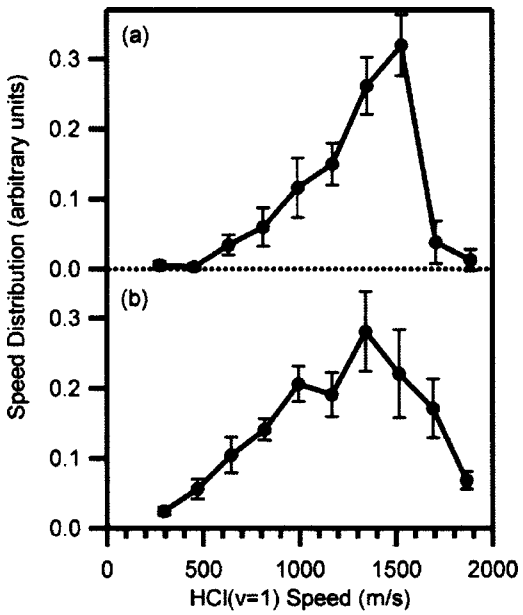

FIG. 5. Speed distributions of the $HCl(v=1,J=0/2)$ product from the reaction of Cl with (a) $CH_2D_2|1100\rangle$ and (b) $CH_2D_2|2000\rangle^-$. The error bars represent σ_{n-1} of replicate measurements.

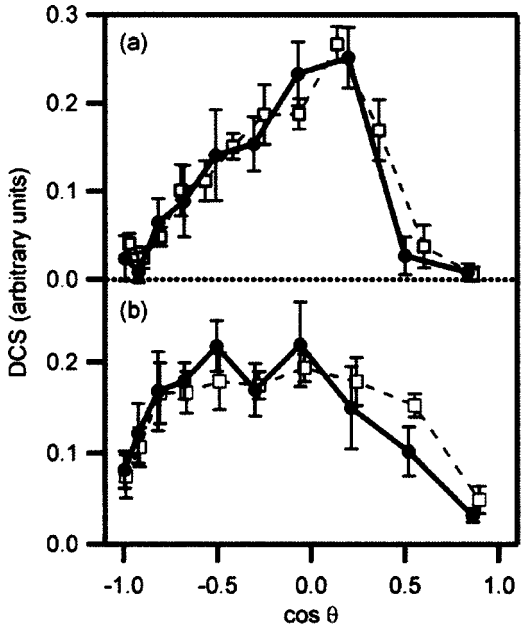

FIG. 6. (a) Comparison of the differential cross sections for the $Cl+CH_2D_2|1100\rangle$ reaction (solid circles) with the $Cl+CH_4|1100,F_2\rangle$ reaction (open squares). (b) Comparison of the differential cross sections for the $Cl+CH_2D_2|2000\rangle^-$ reaction (solid circles) with the $Cl+CHD_3|2000,A_1\rangle$ reaction (open squares). The error bars represent σ_{n-1} of replicate measurements.

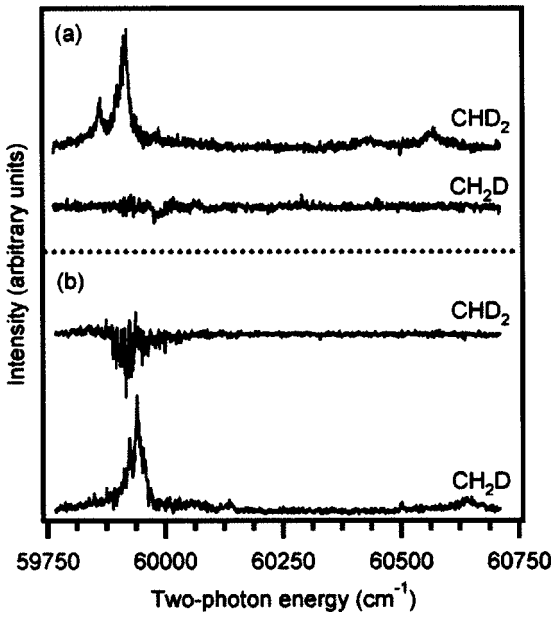

FIG. 7. (a) $2+1$ REMPI spectra of the CHD_2 and CH_2D products obtained simultaneously for the $Cl+CH_2D_2|2000\rangle^-$ reaction. Excitation of the C–H stretch produces only H-abstraction products, HCl and CHD_2. (b) $2+1$ REMPI spectra of the CHD_2 and CH_2D products obtained simultaneously for $Cl+CH_2D_2|0020\rangle^-$ reaction. Excitation of the C–D stretch produces only D-abstraction products, DCl and CH_2D. The increased noise and slight negative signal in the CHD_2 spectrum is a result of depletion of the ground state reaction, $Cl+CH_2D_2$.

products. Although the CHD_2 REMPI spectrum of the $Cl+CH_2D_2|1100\rangle$ reaction indicates that a significant amount of C–H stretch excited CHD_2 is produced, the spatial anisotropy of the $HCl(v=1)$ product suggests that a majority of the $HCl(v=1)$ products are produced in coincidence with $CHD_2(\nu_4=1)$. With this assumption, we convert the speed distribution into the DCS shown in Fig. 6(a). For the $Cl+CH_2D_2|2000\rangle^-$ reaction, the measured spatial anisotropy and the CHD_2 REMPI spectrum indicate that the CHD_2 co-product is produced primarily in the ground state or in the OPLA bending mode. The conversion of the speed distribution into the DCS, however, does not change significantly if the $HCl(v=1)$ products are produced with ground-state CHD_2 or OPLA bend-excited CHD_2 because the OPLA mode is low-frequency ($\sim$510 cm^{-1}). Therefore, we have chosen to include any ambiguities of the co-product state in the error bars of the DCS, as shown in Fig. 6(b). A more proper treatment of the uncertainty would lead to horizontal error bars,[46] but for clarity this approach has not been presented here.

The $HCl(v=1)$ angular distribution for the $Cl+CH_2D_2|1100\rangle$ reaction is peaked in the side-scattered region and has a sharp cutoff at $\cos\theta=0.6$ in the forward-scattered region, whereas the $HCl(v=1)$ angular distribution for the $Cl+CH_2D_2|2000\rangle^-$ reaction is broadly side-scattered. These results represent, to our knowledge, the first observation of a change in scattering dynamics caused by the excitation of two different nearly isoenergetic vibrations in the same molecule. Analogous behavior has been seen in the reactions of chlorine with other vibrationally excited isotopomers of methane, namely $CH_4|1100,F_2\rangle$ and $CHD_3|2000,A_1\rangle$. These reactions were examined by Kim *et al.*[39,47] under similar conditions and are described in detail elsewhere. As shown in Fig. 6, the $HCl(v=1)$ DCS of the $Cl+CH_4|1100,F_2\rangle$ reaction has a sharp cutoff at $\cos\theta=0.6$ and is nearly identical to the $HCl(v=1)$ DCS of the $Cl+CH_2D_2|1100\rangle$ reaction. Likewise, the $HCl(v=1)$ DCS of the $Cl+CHD_3|2000,A_1\rangle$ reaction shows the same broad side-scattering as the $Cl+CH_2D_2|2000\rangle^-$ reaction.

The scattering distributions suggest that the reaction mechanisms of the $Cl+CH_2D_2|1100\rangle$ and $Cl+CH_4|1100,F_2\rangle$ reactions are similar to each other, but different from the $Cl+CH_2D_2|2000\rangle^-$ and $Cl+CHD_3|2000,A_1\rangle$ reactions. This hypothesis is supported by the additional similarities between the $Cl+CH_2D_2|1100\rangle$ and $Cl+CH_4|1100,F_2\rangle$ reactions and between the $Cl+CH_2D_2|2000\rangle^-$ and $Cl+CHD_3|2000,A_1\rangle$ reactions. Both the $Cl+CH_2D_2|1100\rangle$ and $Cl+CH_4|1100,F_2\rangle$ reactions produce significant amounts of stretch-excited methyl radical with little to no ground-state methyl radical and have extremely cold $HCl(v=1)$ rotational distributions.[24,39] On the other hand, both the $Cl+CH_2D_2|2000\rangle^-$ and $Cl+CHD_3|2000,A_1\rangle$ reactions produce predominantly ground-state methyl radical and have warmer $HCl(v=1)$ rotational distributions. We discuss possible reaction mechanisms for the $Cl+CH_2D_2|1100\rangle$ and $Cl+CH_2D_2|2000\rangle$ reactions below.

D. Bond selectivity

Figure 7(a) presents the methyl radical REMPI spectra of the H-abstraction (CHD_2) and D-abstraction (CH_2D) products from the $Cl+CH_2D_2|2000\rangle^-$ reaction in which the

overtone of the C–H stretch is excited. Figure 7(b) presents the corresponding REMPI spectra of the two product channels from the $Cl+CH_2D_2|0020\rangle^-$ reaction, in which the overtone of the C–D stretch is excited. In both figures, the CHD_2 and CH_2D product channels are obtained simultaneously by gating the appropriate mass in the TOF spectrometer. The slight blue shift of the CH_2D bands relative to the CHD_2 bands is caused by the differences in vibrational frequencies of the electronic ground and excited states of the methyl radicals.

From Fig. 7(a), it is clear that excitation of the C–H stretch leads exclusively to H-abstraction products. The D-abstraction product signal (CH_2D^+) is below our detection limit. Likewise, Fig. 7(b) shows that excitation of the C–D stretch leads exclusively to D-abstraction products. The noise in the CHD_2 channel results from the reaction of Cl with ground-state CH_2D_2, which has been subtracted by modulating the IR excitation source. The slight negative signal indicates that the IR excitation is depleting the ground-state reaction. The determination of population, and consequently an accurate branching ratio, is difficult to obtain because of the unknown predissociation rates and Franck–Condon factors in the methyl radical $3p\,^2B_1-X\,^2B_1$ REMPI transitions. However, assuming that the predissociation rates and signal strengths of CH_2D and CHD_2 are equal, the selective excitation of the $|2000\rangle^-$ C–H stretching motion results in the favoring of H-abstraction over D-abstraction by at least a factor of 20. The depletion signal associated with the C–D excitation further complicates the calculation of an accurate branching ratio between the CH_2D and the CHD_2 products. Nevertheless, we estimate that excitation of the $|0020\rangle^-$ C–D-stretching motion favors the D-abstraction channel over the H-abstraction channel by at least a factor of 10.

IV. DISCUSSION

The preceding results show that vibrational excitation of CH_2D_2 significantly influences the dynamics of the $Cl+CH_2D_2$ reaction, causing the $Cl+CH_2D_2|1100\rangle$ and the $Cl+CH_2D_2|2000\rangle^-$ reactions to have different rotational, vibrational, and scattering distributions. We believe that these differences can be qualitatively explained by assuming that the methyl radical product is a spectator and that the $|2000\rangle^-$ mode leads to a wider cone of acceptance for the reaction than the $|1100\rangle$ mode. We discuss these simple models in more detail below.

A. The methyl radical is a spectator

The bond selectivity and mode selectivity demonstrated in the methyl radical vibrational spectrum suggest that the spectator model for the reaction is valid: the chlorine atom interacts with a single C–H oscillator and the remainder of the methane molecule does not participate in the reaction. In the $Cl+CH_2D_2|1100\rangle$ reaction, the chlorine atom reacts with one of the vibrating C–H bonds and leaves the other C–H bond in a stretching motion. In the $Cl+CH_2D_2|2000\rangle^-$ reaction, the chlorine atom reacts with the single stretching C–H oscillator, abstracts all the vibrational energy, and leaves the methyl radical product in the ground state. Figure 8 gives a schematic representation of this mechanism. Similar behavior was observed in the in the $H+H_2O$ and $Cl+H_2O$ reactions by Crim and co-workers.[9,10]

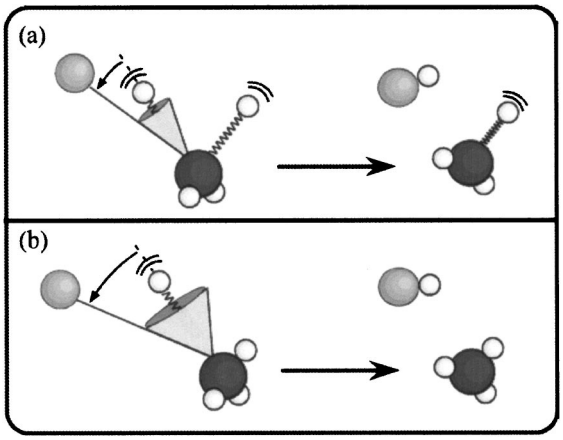

FIG. 8. Spectator model and cone of acceptance diagram. (a) The $Cl+CH_2D_2|1100\rangle$ reaction produces C–H excited methyl radical and has a narrower cone of acceptance than (b) the $Cl+CH_2D_2|2000\rangle^-$ reaction, which produces ground state methyl radical.

The $Cl+CH_2D_2$ reaction is different from the $Cl+H_2O$ reaction because one of the products is a polyatomic molecule. Consequently, different vibrational motions may be excited in the methyl radical product—a behavior that is not possible in the products from the $Cl+H_2O$ reaction. Indeed, we observe a non-negligible amount of the OPLA bending (ν_4) excitation in the CHD_2 products from both the $Cl+CH_2D_2|1100\rangle$ and $Cl+CH_2D_2|2000\rangle^-$ reactions. A simple spectator model cannot explain these bend-excited products. One possible source of the bend excitation is the transformation of the methyl radical from a pyramidal geometry to planar geometry around the transition state region. If this mechanism were dominant, we would expect the $HCl(v=0)$ and $HCl(v=1)$ co-products of the bend excited methyl radical to be formed in the same ratio as the overall reaction. In the $Cl+CH_4|1100,F_2\rangle$ reaction, Kim *et al.*[39] determined that the bend excited methyl radical products were produced predominantly with $HCl(v=1)$ products, indicating that another mechanism was responsible for the excitation of the bending mode. They attributed the formation of bend-excited products to the nonadiabatic interaction of the bending motion in methane with the bending motion in methyl radical. The $HCl(v=1)+CH_3(\nu_2=1)$ channel requires energy flow from one C–H($v=1$) bond to another C–H($v=1$) bond; otherwise only C–H stretch excited CH_3 would be observed. If the bending motion of methane mediates this vibrational energy flow between the two bonds, then the observed $HCl(v=1)+CH_3(\nu_2=1)$ channel could be a reflection of nonadiabatic interaction between the CH_4 bending and CH_3 bending modes during the reaction.

For a majority of the products, the observed bond selectivity and mode selectivity in the reactions of Cl atom with $CH_2D_2|1100\rangle$, $CH_2D_2|2000\rangle^-$, and $CH_2D_2|0020\rangle^-$ indicate that the prepared vibrational mode remains localized in a well-defined motion during the time scale of the reaction. The approach of the Cl atom does not cause significant mode mixing between the C–H and C–D oscillators by breaking

the molecular symmetry, or more precisely, does not cause significant transfer between the C–H and C–D stretches. The lack of this mixing is attributed to the large frequency differences between the C–H and C–D stretching oscillators, ~3000 and 2200 cm^{-1}, respectively.

Halonen and Child[48] note that a sufficiently large bond anharmonicity will quench the interbond coupling on moving to higher overtone states, creating more local mode character in molecules like CH_4. Recently, Halonen[49] modeled the overtone spectrum of CH_4 up to 6050 cm^{-1} by including Fermi resonances in local mode theory. His results indicate that the first overtones of CH_4 can be described in terms of local modes with some bending character. Our data on the $Cl+CH_2D_2$ reaction suggest that the localized character of the first overtone of C–H stretching is dominant as well.

B. $CH_2D_2|2000^-\rangle$ has a larger cone of acceptance than $CH_2D_2|1100\rangle$

The HCl($v=1,J$) rotational distributions from the $Cl+CH_2D_2|1100\rangle$ and the $Cl+CH_2D_2|2000\rangle^-$ excited reactions are both cold, yet they are distinctly different from each other. The cold rotational distributions from H-abstraction reactions of atomic chlorine with various hydrocarbons have often been attributed to a linear transition state, which generates little torque during an impulsive release.[43] Theoretical calculations on the $Cl+CH_4$ reaction have also indicated a linear transition state, thereby supporting this explanation.[50,51] Experimental evidence on the $Cl+C_2H_6$ reaction, however, indicates that cold rotational distributions could also result from products formed with little or no impulsive release.[44]

The recent model of Picconatto *et al.*[52] proposes a third and alternative explanation of the observed cold rotational distributions from reactions of atomic chlorine with hydrocarbons: the rotational distribution is dominated by kinematic constraints and is not a consequence of dynamical effects. The model suggests that the total energy of suprathreshold reactions is not available to the internal energy of the products. Instead, this model posits that a ''reflection'' off the repulsive wall of the potential energy surface limits the available energy. Applying this model to the $Cl+CH_2D_2$ system lowers the available energy for rotation in the HCl($v=1$) products from 3800 to 2500 cm^{-1}. Using this modified E_{avail}, the average energy in rotation is ~8% and ~14% for the $Cl+CH_2D_2|1100\rangle$ and $Cl+CH_2D_2|2000\rangle^-$ reactions, respectively. Although the observed rotational distributions are within the proposed kinematic limit of the model, the energy deposited into rotation is still relatively small. Furthermore, the $Cl+CH_2D_2|1100\rangle$ and the $Cl+CH_2D_2|2000\rangle^-$ reactions have strikingly different rotational distributions, despite having identical kinematics. Consequently, we believe that dynamical effects must play an important role in determining the rotational distribution of the $Cl+CH_2D_2$ reaction products.

In previous studies of the $Cl+CH_4|1100,F_2\rangle$ reaction, Kim *et al.*[39] concluded that the HCl($v=1$) products are formed from collisions that occur at high impact parameter and that have an impulsive energy release along the line of centers. This conclusion was based on a cold rotational distribution, modeling of experimental DCSs, and HCl($v=1,J=1$) alignment data. The model assumes (1) direct, localized reactivity of the polyatomic reagent; (2) a narrow cone of acceptance around the reactive bond; and (3) an impulse release along the line-of-centers. Reactions that exhibit peripheral dynamics,[53–55] that is, reactions that occur at high impact parameters, typically exhibit forward scattering. Incorporating an impulsive energy release into the model causes this typical forward-scattering behavior to shift towards the observed side-scattering behavior. The sharp cutoff at $\cos\theta=0.6$ in the product HCl($v=1$) DCS of the $Cl+CH_4|1100,F_2\rangle$ reaction is a characteristic signature of an impulse release. An impulse release along the line of centers is also consistent with the cold rotational distribution observed for the HCl($v=1$) products. Based on the similar rotational distributions and the DCSs of the HCl($v=1$) products from the $Cl+CH_4|1100,F_2\rangle$ and $Cl+CH_2D_2|1100\rangle$ reactions, we believe that the HCl($v=1$) products from the $Cl+CH_2D_2|1100\rangle$ reaction are formed from collisions that occur at high impact parameter and that have an impulsive energy release along the line of centers.

In contrast, the DCSs of the HCl($v=1$) products from the $Cl+CH_2D_2|2000\rangle^-$ and the $Cl+CHD_3|2000,A_1\rangle$ reactions do not have the sharp cutoffs at $\cos\theta=0.6$ that dominate the DCSs of the $Cl+CH_2D_2|1100\rangle$ and $Cl+CH_4|1100,F_2\rangle$ reactions. Instead, the DCSs of these reactions are more broadly side-scattered. We believe that these reactions also exhibit peripheral dynamics and have an impulse release, but the impulse is no longer restricted to be along the line of centers. Because more vibrational energy is localized into a single C–H oscillator, the transition state region of the $Cl+CH_2D_2|2000\rangle^-$ reaction is believed to deviate from linearity, allowing a wider cone of acceptance for the reaction. As a consequence, the sharp cutoff that signifies an impulse release is blurred over more angles, as seen in the HCl($v=1$) DCSs of the $Cl+CHD_3|2000,A_1\rangle$ and $Cl+CH_2D_2|2000\rangle^-$ reactions. Moreover, this wider cone of acceptance should allow for a larger torque to be exerted on the HCl($v=1$) product during the impulse release, resulting in more rotational excitation. This model successfully explains the rotational distribution of the $Cl+CH_2D_2|2000\rangle^-$ reaction shown in Fig. 3(b). Figure 8 depicts the wider cone of acceptance for the $Cl+CH_2D_2|2000\rangle^-$ reaction as compared to the $Cl+CH_2D_2|1100\rangle$ reaction.

V. CONCLUSIONS

We have observed strong bond and mode selectivity in the $Cl+CH_2D_2$ reaction both in the product distribution and the scattering dynamics. Excitation of the first overtone of the C–H and C–D stretches leads to dramatic bond selectivity; within our measurement uncertainty, excitation of the C–H stretch leads exclusively to H-abstraction products, whereas excitation of the C–D stretch leads exclusively to D-abstraction products. In addition, the excitation of two nearly isoenergetic but distinct C–H stretching motions displays striking differences in the rotational distribution, the vibrational distribution, and the scattering angle of the

reaction products. The $Cl+CH_2D_2|1100\rangle$ reaction yields primarily stretch excited methyl radical, whereas the $Cl+CH_2D_2|2000\rangle^-$ reaction yields ground-state methyl radical. These results suggest that the Cl atom interacts with an individual C–H oscillator and treats the rest of the molecule as an innocent bystander. The warmer rotational distribution and the more broadly side-scattered DCS of the $Cl+CH_2D_2|2000\rangle^-$ reaction suggest that it has a larger cone of acceptance than the $Cl+CH_2D_2|1100\rangle$ reaction.

The striking bond selectivity and mode selectivity observed in the $Cl+CH_2D_2$ reaction show that the prepared vibrational motion remains localized during the timescale of the reaction. These experiments represent an extension of vibrational control to systems containing larger molecules, where the additional vibrational degrees of freedom could result in intramolecular vibrational redistribution. We believe our results to be the first example of mode selectivity observed in the angular distribution of the reaction products. Thus, vibrational energy can be used to direct the scattering angle of the products as well as control which products are formed. We believe that vibrational excitation can be successfully applied to reaction systems that have localized vibrations, direct reactions, and vibrational motions that map onto the reaction coordinate.

ACKNOWLEDGMENTS

Two of the authors (H.A.B. and J.P.C.) thank the National Science Foundation for graduate fellowships. H.A.B. also acknowledges Stanford University for the award of a Stanford Graduate Fellowship. This material is based upon work supported by the National Science Foundation under Grant No. 0242103.

[1] F. F. Crim, J. Phys. Chem. **100**, 12725 (1996).
[2] R. N. Zare, Science **279**, 1875 (1998).
[3] F. F. Crim, Acc. Chem. Res. **32**, 877 (1999).
[4] J. C. Polanyi and W. H. Wong, J. Chem. Phys. **51**, 1439 (1969).
[5] M. H. Mok and J. C. Polanyi, J. Chem. Phys. **51**, 1451 (1969).
[6] B. A. Hodgson and J. C. Polanyi, J. Chem. Phys. **55**, 4745 (1971).
[7] D. S. Perry, J. C. Polanyi, and J. C. W. Wilson, Chem. Phys. **3**, 317 (1974).
[8] A. Sinha, M. C. Hsiao, and F. F. Crim, J. Chem. Phys. **92**, 6333 (1990).
[9] A. Sinha, M. C. Hsiao, and F. F. Crim, J. Chem. Phys. **94**, 4928 (1991).
[10] A. Sinha, J. D. Thoemke, and F. F. Crim, J. Chem. Phys. **96**, 372 (1992).
[11] R. B. Metz, J. D. Thoemke, J. M. Pfeiffer, and F. F. Crim, J. Chem. Phys. **99**, 1744 (1993).
[12] J. D. Thoemke, J. M. Pfeiffer, R. B. Metz, and F. F. Crim, J. Phys. Chem. **99**, 13748 (1995).
[13] J. M. Pfeiffer, E. Woods, R. B. Metz, and F. F. Crim, J. Chem. Phys. **113**, 7982 (2000).
[14] M. J. Bronikowski, W. R. Simpson, B. Girard, and R. N. Zare, J. Chem. Phys. **95**, 8647 (1991).
[15] M. J. Bronikowski, W. R. Simpson, and R. N. Zare, J. Phys. Chem. **97**, 2204 (1993).
[16] M. J. Bronikowski, W. R. Simpson, and R. N. Zare, J. Phys. Chem. **97**, 2194 (1993).
[17] R. B. Metz, J. M. Pfeiffer, J. D. Thoemke, and F. F. Crim, Chem. Phys. Lett. **221**, 347 (1994).
[18] J. M. Pfeiffer, R. B. Metz, J. D. Thoemke, E. Woods, and F. F. Crim, J. Chem. Phys. **104**, 4490 (1996).
[19] C. Kreher, R. Theinl, and K.-H. Gericke, J. Chem. Phys. **104**, 4481 (1996).
[20] C. Kreher, J. L. Rinnenthal, and K.-H. Gericke, J. Chem. Phys. **108**, 3154 (1998).
[21] D. Troya, I. Banos, M. Gonzalez, G. Wu, M. A. ter Horst, and G. C. Schatz, J. Chem. Phys. **113**, 6253 (2000).
[22] D. Troya, M. Gonzalez, G. Wu, and G. C. Schatz, J. Phys. Chem. A **105**, 2285 (2001).
[23] D. J. Nesbitt and R. W. Field, J. Phys. Chem. **100**, 12735 (1996).
[24] Z. H. Kim, H. A. Bechtel, and R. N. Zare, J. Am. Chem. Soc. **123**, 12714 (2001).
[25] S. Yoon, R. J. Holiday, and F. F. Crim, J. Chem. Phys. **119**, 4755 (2003).
[26] R. D. Beck, P. Maroni, D. C. Papageorgopoulos, T. T. Dang, M. P. Schmid, and T. R. Rizzo, Science **308**, 98 (2003).
[27] J. L. Duncan and M. M. Law, Spectrochim. Acta, Part A **53**, 1445 (1997).
[28] V. M. Blunt, N. Mina-Camilde, D. L. Cedeno, and C. Manzanares, Chem. Phys. **209**, 79 (1996).
[29] R. Atkinson, D. L. Baulch, R. A. Cox, J. R. F. Hampson, J. A. Kerr, and J. Troe, J. Phys. Chem. Ref. Data **21**, 1125 (1992).
[30] W. B. DeMore, S. P. Sander, C. J. Howard, A. R. Ravishankara, D. M. Golden, C. E. Kolb, R. F. Hampson, M. J. Kurylo, and M. J. Molina, ''Chemical kinetics and photochemical data for use in stratospheric modeling,'' evaluation number 12; JPL publication 97-4; Jet Propulsion Laboratory, Pasadena, CA, 1997.
[31] J. C. Corchado, D. G. Truhlar, and J. Espinosa-Garcia, J. Chem. Phys. **112**, 9375 (2000).
[32] G. D. Boone, F. Agyin, D. J. Robichaud, F.-M. Tao, and S. A. Hewitt, J. Phys. Chem. A **105**, 1456 (2001).
[33] W. R. Simpson, A. J. Orr-Ewing, T. P. Rakitzis, S. A. Kandel, and R. N. Zare, J. Chem. Phys. **103**, 7299 (1995).
[34] W. R. Simpson, T. P. Rakitzis, S. A. Kandel, A. J. Orr-Ewing, and R. N. Zare, J. Chem. Phys. **103**, 7313 (1995).
[35] P. C. Samartzis, B. Bakker, T. P. Rakitzis, D. H. Parker, and T. N. Kitsopoulos, J. Chem. Phys. **110**, 5201 (1999).
[36] A. Yokoyama and T. Takayanagi, Chem. Phys. Lett. **307**, 48 (1999).
[37] E. A. Rohlfing, D. W. Chandler, and D. H. Parker, J. Chem. Phys. **87**, 5229 (1987).
[38] J. L. Brum, R. D. Johnson III, and J. W. Hudgens, J. Chem. Phys. **98**, 3732 (1993).
[39] Z. H. Kim, H. A. Bechtel, and R. N. Zare, J. Chem. Phys. **117**, 3232 (2002).
[40] S. G. Westre, X. Liu, J. D. Getty, and P. B. Kelly, J. Chem. Phys. **95**, 8793 (1991).
[41] D. W. Chandler, J. W. Thoman Jr., M. H. M. Janssen, and D. H. Parker, Chem. Phys. Lett. **156**, 151 (1989).
[42] J. Zhou, J. J. Lin, and K. Liu, J. Chem. Phys. **119**, 8289 (2003).
[43] W. R. Simpson, T. P. Rakitzis, S. A. Kandel, T. LevOn, and R. N. Zare, J. Phys. Chem. **100**, 7938 (1996).
[44] S. A. Kandel, T. P. Rakitzis, T. LevOn, and R. N. Zare, J. Chem. Phys. **105**, 7550 (1996).
[45] S. Rudic, C. Murray, D. Ascenzi, H. Anderson, J. N. Harvey, and A. J. Orr-Ewing, J. Chem. Phys. **117**, 5692 (2002).
[46] S. A. Kandel, T. P. Rakitzis, T. LevOn, and R. N. Zare, Chem. Phys. Lett. **265**, 121 (1997).
[47] Z. H. Kim, Ph.D. thesis, Stanford University, 2002.
[48] L. Halonen and M. S. Child, Mol. Phys. **46**, 239 (1982).
[49] L. Halonen, J. Chem. Phys. **106**, 831 (1997).
[50] T. N. Truong, D. G. Truhlar, K. K. Baldrige, M. S. Gordon, and R. Steckler, J. Chem. Phys. **90**, 7137 (1989).
[51] K. D. Dobbs and D. A. Dixon, J. Phys. Chem. **98**, 12584 (1994).
[52] C. A. Picconatto, A. Srivastava, and J. J. Valentini, J. Chem. Phys. **114**, 1663 (2001).
[53] P. M. Aker and J. J. Valentini, Isr. J. Chem. **30**, 157 (1990).
[54] M. Ben-Nun, M. Brouard, J. P. Simons, and R. D. Levine, Chem. Phys. Lett. **210**, 423 (1993).
[55] X. Wang, M. Ben-Nun, and R. D. Levine, Chem. Phys. **197**, 1 (1995).
[56] W. J. van der Zande, R. Zhang, R. N. Zare, K. G. McKendrick, and J. J. Valentini, J. Phys. Chem. **95**, 8205 (1991).